Volume 1 | Number 1 | Jan 2013 | Pages 1–100

Nanoscale

www.rsc.org/nanoscale

ROYAL SOCIETY OF CHEMISTRY

www.rsc.org/nanoscale

Flexoelectric MEMS: towards an electromechanical strain diode

U.K.Bhaskar[a+*], N.Banerjee[b+], A.Abdollahi[a], E.Solanas[d], G.Rijnders[b], and G.Catalan[a,c*]

Abstract here. Piezoelectricity and flexoelectricity are two independent, but not incompatible, forms of electromechanical response exhibited by nanoscale ferroelectrics. Here, we show that flexoelectricity can either enhance or suppress the piezoelectric response of the cantilever depending on the ferroelectric polarity and lead to an asymmetric (two-state) electromechanical response.

The non-centrosymmetric lattice of piezoelectric materials responds to elastic deformations by generating a dielectric polarization. Piezoelectricity allows non-centrosymmetric crystals to efficiently transduce electrical energy into mechanical energy and vice versa. In most microelectromechanical systems (MEMS)[1,2], piezoelectric materials are used together with a non-piezoelectric elastic layer in a composite structure, referred to hereon as a bimorph structure. The mechanical clamping induced by the nonpiezoelectric layer helps translate the homogenous piezoelectric strains generated on application of an electrical bias (converse piezoelectricity) into a flexural motion: the region of the piezoelectric closest to the interface with the inert material deforms less than the region furthest away, thereby creating a deformation gradient and hence a bending.

Meanwhile, converse flexoelectricity[3,4,5,6,7,8,9] is a different electromechanical coupling that also allows any insulating material, irrespective of its symmetry, to bend in response to an applied voltage. Flexoelectric bending arises from deformation at the unit cell level[6] and does not require any clamping layer. Flexoelectricity is not inherently incompatible with piezoelectricity, so in piezoelectric bimorph actuators flexoelectric bending must exist in addition to the piezoelectric bending. However, flexoelectricity, when compared to piezoelectricity, is a weak effect of little practical significance in *bulk* materials, so its contribution to actuator performance has so far gone unnoticed. In MEMS, however, the balance of power

between piezoelectricity and flexoelectricity is shifted, because any (strain) gradient scales inversely with the thickness, and MEMS can be very thin.

It has been theoretically predicted[10,11] that the interaction between flexoelectricity and piezoelectricity in nanocantilevers can lead to significant size-dependent enhancement of the effective (piezoelectric + flexoelectric) coefficients, a prediction that still awaits experimental verification. There is moreover an additional consideration when the piezoelectric layer is a ferroelectric: the sign of the piezoelectric coefficient (a third rank tensor) can be switched by applying a sufficiently large (coercive) voltage, whereas the sign of flexoelectricity (a fourth rank tensor) is independent of the ferroelectric polarity. Therefore, two distinct regimes of operation should in theory exist: when flexoelectricity and ferroelectricity align opposite to each other, resulting in a decreased or eventually even cancelled deformation, and when they align together, resulting in an enhanced deformation (**Figure 1**(d)). The asymmetry of this interaction has been demonstrated in bulk pyramidal ceramic lead magnesium niobate-lead titanate[12]. This asymmetry offers the possibility of engineering a new type of electromechanical device with inherent two-state functionality, namely, one where the energy cost of mechanical deformation depends on the sign of the ferroelectric polarization. In this paper, by using a $Pb(Zr_{0.52},Ti_{0.48})O_3$ (PZT)-based ferroelectric bimorph MEMS cantilever, we demonstrate that piezoelectric and flexoelectric effects can indeed be combined to achieve such two state functionality in ferroelectric MEMS.

For this work, all-oxide nanocantilevers (**Figure 1**(a,b)) were fabricated as capacitor structures with a PZT active layer sandwiched between two $SrRuO_3$ (SRO) electrodes, and the whole structure is epitaxially grown on a buffer of Yttria-stabilized Zirconia (YSZ) on Si. The fabrication method utilized the lift-off patterning[13] of the epitaxial oxide stack, followed by release of the freestanding devices using anisotropic etching. In contrast to the traditional top-down patterning, the lift-off process employs a sacrificial layer of amorphous AlO_x mask and structures the hetero-epitaxial multilayer in a single lift-off step. All the oxide layers were grown by pulsed laser deposition. The buffer layer of YSZ was utilized to promote the epitaxial

a. *ICN2 – Institut Catala de Nanociencia i Nanotecnologia, CSIC and The Barcelona Institute of Science and Technology, Campus UAB, 08193 Bellaterra (Barcelona), Spain.*
b. *Faculty of Science and Technology and MESA+ Institute for Nanotechnology, University of Twente, P.O. Box 217, 7500 AE Enschede, The Netherlands*
c. *ICREA - Institucio Catalana de Recerca i Estudis Avançats, 08010 Barcelona, Spain*
d. *Lyncée Tec SA, PSE-A, CH-1015 Lausanne, Switzerland.*

growth of the perovskite layers on Si, and it also acted as the elastic layer in the bimorph actuation in the final devices. Following the growth and lift-off patterning of the heterostructures, the top SrRuO$_3$ electrode layer was defined using ion-beam etching. The PZT films are oriented with the perovskite {110} planes parallel to the surface. The dielectric and ferroelectric properties of the PZT films grown under similar conditions are reported in [13,14,15]. At the frequency of measurement (1.3 kHz), the dielectric loss tan(δ) is <0.1, indicating that the released cantilevers are dielectrically sound and not leaky. The final free-standing devices were released by anisotropic etching of the Si (100) substrate employing basic solution[16]. In order to facilitate inference by comparison, piezoelectric bimorph cantilevers were fabricated for two thicknesses of PZT - 150 and 75 nm. In both cases, the thickness of the YSZ elastic layer was the same as that of the piezoelectric layer, while the thickness of top and bottom SRO electrode was 25 nm. Finally, a "flexoelectric amplifier" was made from a 100 nm thick PZT bimorph structure having a thick SRO electrode ~100 nm for the top electrode. The thicker top electrode partially compensates for the non-centrosymmetry introduced by the 100 nm thick YSZ layer and the 25 nm thick SRO bottom electrode. We have created an app that calculates the asymmetry in bending as a function of polarity for any user-specified material coefficients and geometric parameters, so as to allow potential users to design ferroelectric MEMS devices with a desired level of electromechanical asymmetry (https://umeshkbhaskar.shinyapps.io/pzt_app/).

The observation of out-of-plane oscillations (**Figure 1**(c)) induced by applying an electrical excitation to the released cantilevers was made using a commercial Digital Holographic Microscope (DHM)[17,18] working in stroboscopic mode. The displacement (z) was measured on multiple points along the length of the cantilever (supplementary **Figure 1**), and the curvature (κ) calculated as $(\partial^2 z)/(dx^2)$, where x is the horizontal distance to the clamping point.

The curvature of the cantilever, along with the applied sinusoidal excitation, is plotted in F**igure 2** as a function of time, both for the case when the polarization vector is pointing in the positive z axis, referred to heron on as P_+ (colored blue in **Figure 2**(a)), and the opposite case, referred to hereon as P_- (colored red in **Figure 2**(b)). The direction of voltage sweep for both P_+ and P_- is unipolar, and is chosen so as to favor the existing polarization; for example, a sinusoidal excitation spanning only negative voltages is applied to favor P_+. This is done in order to avoid additional electromechanical contributions from switching during voltage application. The curvature as a function of

applied electric field for full bipolar voltage cycle is also shown in **Figure3** (a) for the 150 nm, and (b) 75 nm thick PZT bimorph, showing the characteristic butterfly-like hysteresis loops expected from the switching piezoresponse of a ferroelectric cantilever[19].

For an up-polarized sample P_+, applying a negative voltage at the top electrode increases the ferroelectric polarization, causing an out of plane expansion and in-plane contraction of the ferroelectric layer that results in an *upward* bend of the cantilever (**Figure 1**(d)). Conversely, if the ferroelectric polarization is pointing down P_-, a negative voltage will cause the polarization to decrease in magnitude, thus contracting the ferroelectric layer out-of-plane and expanding it in-plane, which results in a *downward* bend. Meanwhile, the flexoelectrically-induced bending depends only on the sign of the voltage, with a negative voltage resulting in a upward flexoelectric bend because the flexoelectric coefficient for 110-oriented perovskites is negative[20]. Thus, for $P+$ polarity, flexoelectricity and piezoelectricity both try to bend the cantilever upwards as a function of increasing voltage, whereas for $P-$ polarity flexoelectricity partially offsets piezoelectricity. As a result, the slope $\partial\kappa/\partial V$ must be bigger for $P+$ than for $P-$.

We can calculate this effect analytically. The first step is to determine the z position of the torque neutral axis (z_m), a concept well known in engineering mechanics[21,22], which is defined as the weighted centre (z_i) of the product of Young's modulus (E_i) and cross-sectional area (A_i) for all i layers in the bimorph structure:

$$z_m = \frac{\sum_i z_i E_i A_i}{\sum_i E_i A_i}$$

(1)

$\frac{\partial\kappa}{\partial V}$ can now be expressed as[23]:

$$\frac{\partial\kappa}{\partial V} = \frac{E_p Z_p d_{31}}{\sum_i E_i t_i (\frac{t_i^2}{12} + Z_i^2)},$$

(2)

where, E_p is the Young's modulus of the PZT layer, t_i is thickness of layer i, Z_i is the position of the centre of layer i with respect to the neutral axis, and d_{31} is the intrinsic piezoelectric coefficient. Assuming a flexoelectric coefficient μ_{12}, the numerator in Eq (2) can be explicitly expanded as $E_p Z_p d_{31} + \mu_{12}$ for $P+$, and $E_p Z_p d_{31} - \mu_{12}$ for $P-$. Thus, $\frac{\partial\kappa}{\partial V}$ can now be expressed as

COMMUNICATION

$$\frac{\partial \kappa}{\partial V} = \frac{E_p Z_p d_{31}{}^{eff}}{\sum_i E_i t_i (\frac{t_i^2}{12} + Z_i^2)},$$

(3)

where,

$$d_{31}{}^{eff} = d_{31} \pm \frac{\mu_{12}}{E_p Z_p}.$$

(4)

We see then that the combination of piezoelectricity (d_{31}) and flexoelectricity (μ_{12}) yields a polarity-dependent value of the effective piezoelectricity ($d_{31}{}^{eff}$). This asymmetry is size-dependent, because the flexoelectric contribution (second term on the right side of eq. 4) scales in inverse proportion to Z_p. Though we have calculated it analytically for cantilevers, the existence and size dependence of piezoelectric asymmetry is a more general principle that applies even to bulk piezoelectric devices [12]. In **Figure 4(a),** we plot the curvature as a function of voltage for the 150 nm thick PZT bimorph structure, using only the data from the reverse sweeps of P_+ and P_-, which corresponds to the electromechanical response from the poled states[19], and compare the $d_{31}{}^{eff}$ coefficient extracted from the slope κ/V for each polarization direction. The effective $d_{31}{}^{eff}$ coefficients extracted using Eq(3) are 27.38 ± 0.08 pm/V and 28.89 ± 0.07 pm/V for *P-* and *P+* respectively, which is comparable to prior measurements on PZT cantilevers[24,23]. The asymmetry in $d_{31}{}^{eff}$ is 5.36%. Using Eq(4), we can use this asymmetry to calculate the flexoelectric coefficient, obtaining μ_{12}=12.42 ± 0.05 nC m[-1]. Experimentally the flexoelectric coefficient of PZT is an unknown and cannot be compared, but the measured values are in good agreement with theoretical prdictions[4,25]. We arrive at comparable values of 26.49 pm/V and 27.95 pm/V for the effective piezoelectric constants and a comparable value of μ_{12}=11.25 ± 0.05 nC m[-1] for the flexoelectric coefficient if we use a self-consistent continuum model for our cantilevers [8].

In order to verify that the observed asymmetry in piezoelectric coefficients is due to flexoelectricity, we have conducted the same set of measurements on a PZT bimorph structure but with half the thickness for both the PZT film (75 nm), and the elastic layer (75 nm). The thickness of top and bottom SRO electrodes is still 25 nm. In **Figure 4** (b), we plot the κ-E for the 75 nm thick PZT bimorph. In this case, the measured $d_{31}{}^{eff}$ coefficients are 24.24 ± 0.05 pm/V and 27.56 ± 0.08 pm/V for *P-* and *P+* respectively. The asymmetry is 12.81%: over twice as much as for the twice-as-thick cantilever, as expected from eq. (4). The calculated flexoelectric coefficient in this case is μ_{12}=12.59 ± 0.03

nC m[-1], almost identical to that of the thicker film, providing further evidence for the flexoelectric origin of the asymmetry.

It is now clear that flexoelectricity induces an asymmetry in the κ-E curve of the PZT bimorph structure; however, to achieve a clear two state functionality, we need the bending moments generated by piezoelectricity and flexoelectricity to be of comparable magnitude. One way would be to further reduce the thickness of the flexoelectric layer, but maintaining the integrity of ultra-thin cantilevers is a difficult engineering challenge. Alternatively, we could reduce the thickness of the elastic clamping layer (YSZ), which simultaneously enhances the flexoelectric bending and reduces the piezoelectric one. Again, however, owing to technological issues the scaling of the elastic/template layer is not feasible, as it has a negative impact on the structural quality of the layers grown on top. But there is a third way. By depositing a thicker top electrode of SRO (100 nm), we can partially compensate the clamping asymmetry induced by the YSZ layer (100 nm) + SRO bottom electrode (25nm) on the 100 nm thick PZT bimorph structure.

This moves the torque neutral axis (z_m) of the PZT bimorph closer to the center of the PZT thin film, resulting in comparable magnitudes of the bending moments arising from flexoelectricity and piezoelectricity. In **Figure 5**, we plot the κ-E for the aforementioned device. The measured $d_{31}{}^{eff}$ coefficients show a very large asymmetry ~47%: $d_{31}{}^{eff}(piezo + flexo) = $ 36.85 ± 0.29 pm/V and $d_{31}{}^{eff}(piezo - flexo)$ = 22.61 ± 0.21 pm/V for *P-* and *P+* respectively. The calculated flexoelectric coefficient in this case is μ_{12}=16.53 ± 0.61 nC m[-1], in good correspondence with the other ferroelectric bimorph cantilevers.

Conclusions

The collaboration vs competition dynamic between flexoelectricity and ferroelectricity can thus be exploited not only to enhance the electromechanical performance of cantilevers[10], but to design fundamentally new electromechanical devices. In particular, the presence of flexoelectricity in ferroelectricity dominated actuation allows creating an asymmetric piezoelectricity amplifier, whose effective piezoelectric coefficients are determined by the sign of the ferroelectric polarisation. Alternatively, by tuning the geometry of the bimorph, it would also be possible to realize flexoelectricity dominated actuation, which would strain bi-directionally and display linear electromechanical performance (with different slopes for the opposite polarisation states). Looking beyond

PZT, lead free piezoelectrics like barium titanate (BTO)[26] display much larger flexoelectric coefficients and smaller piezoelectric coefficients. Thus, BTO bimorph structures, operating around the curie temperature, would allow tunability of the full palette of electromechanical functionalities and assymetries on a single device.

References

1   S. H. Baek, J. Park, D. M. Kim, V. a. Aksyuk, R. R. Das, S. D. Bu, D. a. Felker, J. Lettieri, V. Vaithyanathan, S. S. N. Bharadwaja, N. Bassiri-Gharb, Y. B. Chen, H. P. Sun, C. M. Folkman, H. W. Jang, D. J. Kreft, S. K. Streiffer, R. Ramesh, X. Q. Pan, S. Trolier-McKinstry, D. G. Schlom, M. S. Rzchowski, R. H. Blick and C. B. Eom, *Science* 2011, **334**, 958–961.

2   P. Muralt, N. Ledermann, J. Paborowski, a. Barzegar, S. Gentil, B. Belgacem, S. Petitgrand, a. Bosseboeuf and N. Setter, *IEEE Trans. Ultrason. Ferroelectr. Freq. Control*, 2005, **52**, 2276–2288.

3   A. K. Tagantsev and A. S. Yurkov, *J. Appl. Phys.*, 2012, **112**, 044103.

4   P. Zubko, G. Catalan and A. K. Tagantsev, *Annu. Rev. Mater. Res.*, 2013, **43**, 387–421.

5   T. D. Nguyen, S. Mao, Y. W. Yeh, P. K. Purohit and M. C. McAlpine, *Adv. Mater.*, 2013, **25**, 946–974.

6   E. Bursian and N. Trunov, *Sov. Phys. Solid State*, 1974, **16**, 760–762.

7   E. Bursian and O. I. Zaikovskii, *Sov. Phys. Solid State*, 1968, **10**, 1121.

8   A.Abdollahi; C.Peco; D.Millán; M.Arroyo; I.Arias. Computational Evaluation of the Flexoelectric Effect in Dielectric Solids. *J. Appl. Phys* 2014, **116**,*093502*.

9   V. G. Zalesskii and E. D. Rumyantseva, *Phys. Solid State*, 2014, **56**, 1352–1354.

10 M. Majdoub, P. Sharma and T. Çağin, *Phys. Rev. B*, 2008, **78**, 121407.

11 A. Abdollahi. and I. Arias, *J. Appl. Mech*, 2015, **82**, 121003.

12 P. Hana, M. Marvan, L. Burianova, S. J. Zhang, E. Furman and T. R. Shrout, *Ferroelectrics*, 2006, **336**, 137–144.

13 N. Banerjee, G. Koster and G. Rijnders, *Appl. Phys. Lett.*, 2013, **142909**, 0–5.

14 M. D. Nguyen, R. J. A. Steenwelle, J. M. Dekkers, D. H. A. Blank and G. Rijnders, *Nano/Micro Eng. Mol. Syst. 2009. NEMS 2009. 4th IEEE Int. Conf.*, 2009, 649–652.

15 M. Dekkers, M. D. Nguyen, R. Steenwelle, P. M. Riele, D. H. A. Blank and G. Rijnders, *Appl. Phys. Lett.*, 2012, **95**, 012902.

16 N. Banerjee, E. P. Houwman, G. Koster and G. Rijnders, *Apl Mater.*, 2014, **2**, 096103.

17 E. Cuche, Y. Emery and F. Montfort, *Nat. Photonics*, 2009, **3**, 633–635.

18 Y. Cotte, F. Toy, P. Jourdain and N. Pavillon, *Nat. Photonics*, 2013, **7**, 113–117.

19 D. Damjanovic, in *The Science of Hysteresis*, 2006, vol. 3, pp. 337–465.

20 P. Zubko, G. Catalan, a. Buckley, P. Welche and J. Scott, *Phys. Rev. Lett.*, 2007, **99**, 167601.

21 S. H. Crandall, T. J. Lardner and N. C. Dahl, *An introduction to the mechanics of solids: with SI units*, 1999, vol. 3.

22 M. S. Weinberg, *J. Microelectromechanical Syst.*, 1999, **8**, 529–533.

23 M. Dekkers, H. Boschker, M. van Zalk, M. Nguyen, H. Nazeer, E. Houwman and G. Rijnders, *J. Micromechanics Microengineering*, 2013, **23**, 025008.

24 H. Nazeer, M. D. Nguyen, Ö. S. Sukas, G. Rijnders, L. Abelmann and M. C. Elwenspoek, *J. Microelectromech. Syst.*, 2014, **24**, 166–173.

25 G. Catalan, A. Lubk, A. H. G. Vlooswijk, E. Snoeck, C. Magen, A. Janssens, G. Rispens, G. Rijnders, D. H. A. Blank and B. Noheda, *Nat. Mater.*, 2011, **10**, 963–7.

26 J. Narvaez, S. Saremi, J. Hong, M. Stengel and G. Catalan, *Phys. Rev. Lett.*, 2015, **115**, 1–5.
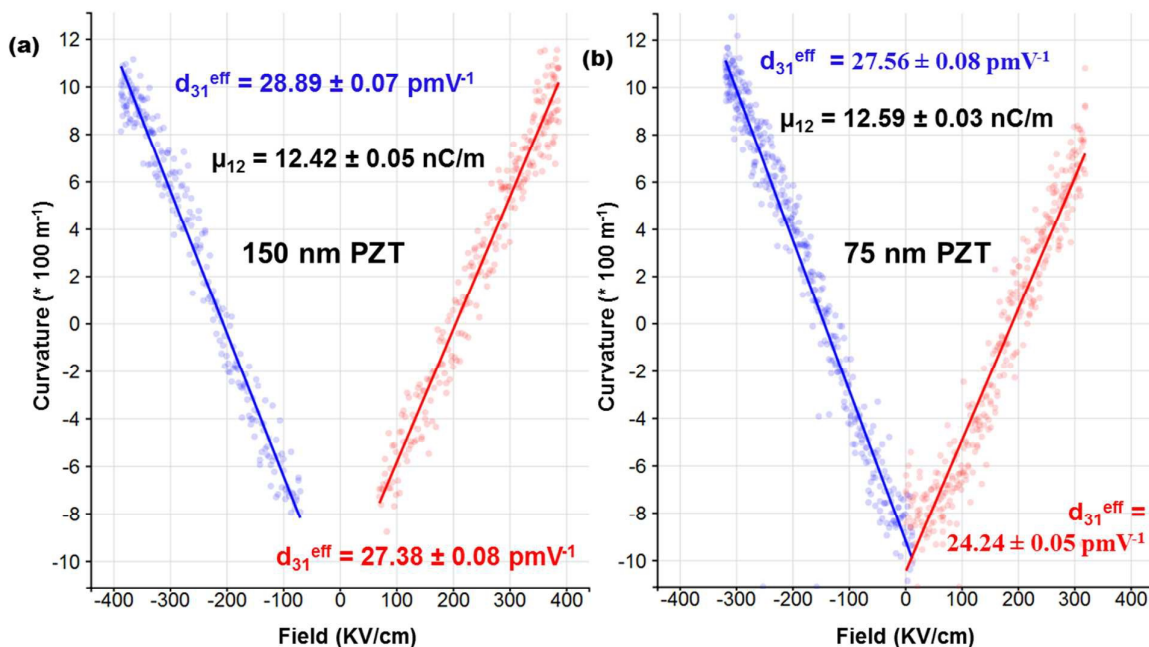
Figures
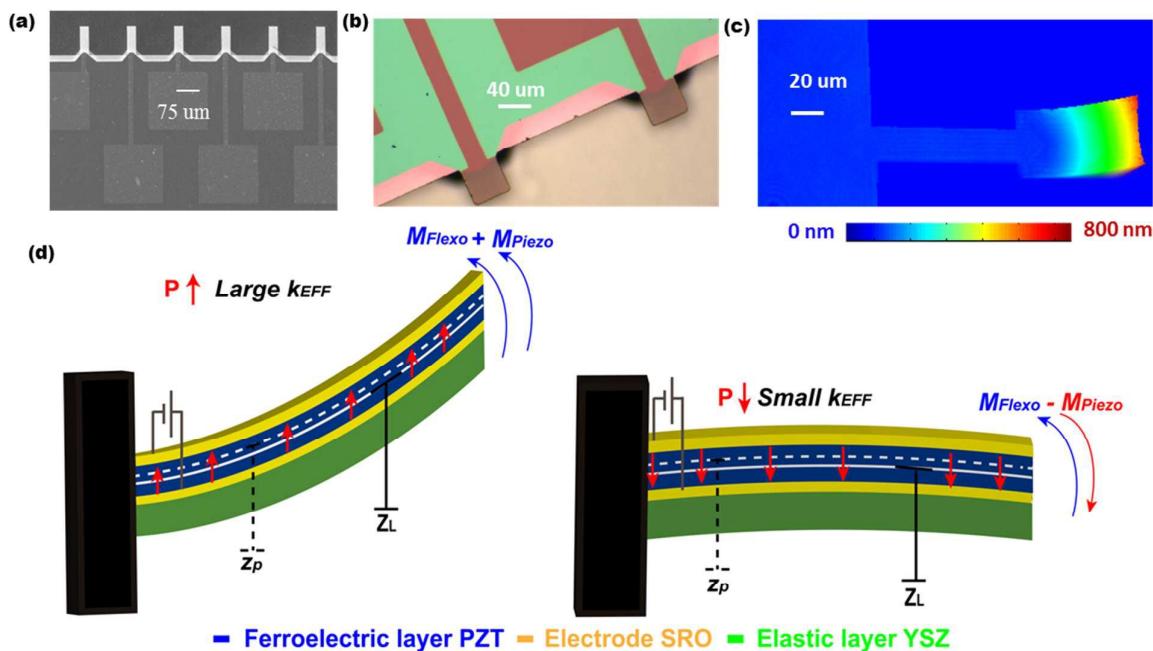
Figure 1(a) Scanning electron microscopy and (b) optical image of an array of PZT nanocantilevers; (c) 3D image of one PZT nanocantilevers with colour scale corresponding to the out of plane displacement; (d) Schematic illustration of piezoelectric and flexoelectric moments working together for ferroelectric polarisation in the negative z axis and cancelling each other for ferroelectric polarisation in the positive z axis.
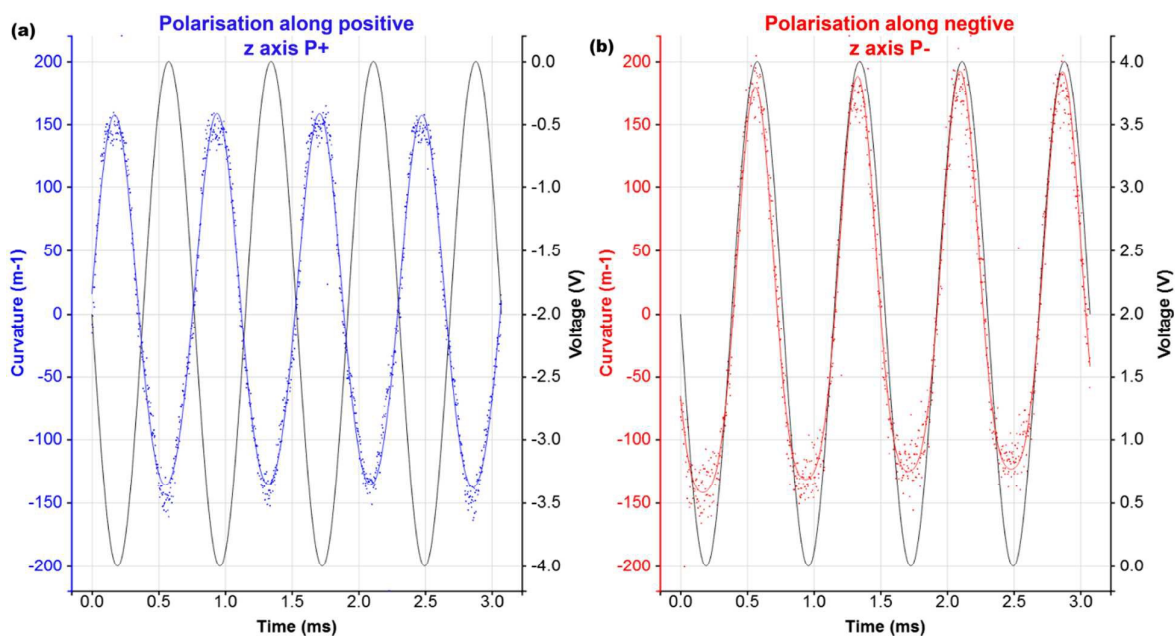

Figure 2 Field-induced oscillations in the curvature of the cantilever, along with the applied sinusoidal voltage excitation (1301 Hz), plotted as a function of the time: (a) for the case when the polarization vector is pointing in the positive z axis - P_+, (b) and the other case when the polarization vector is pointing in the negative z axis - P_-.
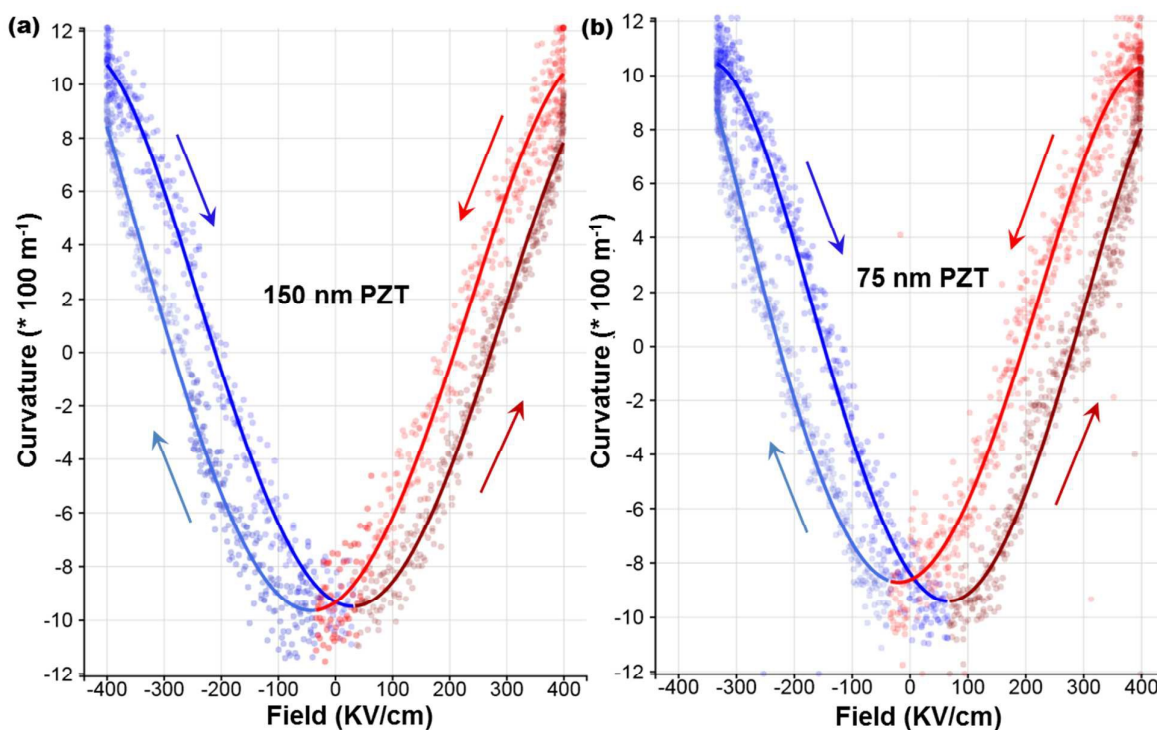
Figure 3 Butterfly hysteresis loops of curvature as a function electric field for (a) 150 nm thick and (b) 75 nm thick PZT bimorph.

Figure 4 (a) Data from reverse sweeps (i.e., poled state) of curvature k as a function of the applied field for the 150 nm and (b) 75 nm thick PZT bimorph. The solid lines are least-square fits, the slope of which is the effective piezoelectric coefficient d_{31}^{eff} (eq.3), from which the flexoelectric coefficient μ_{13} is extracted (eq. 4).
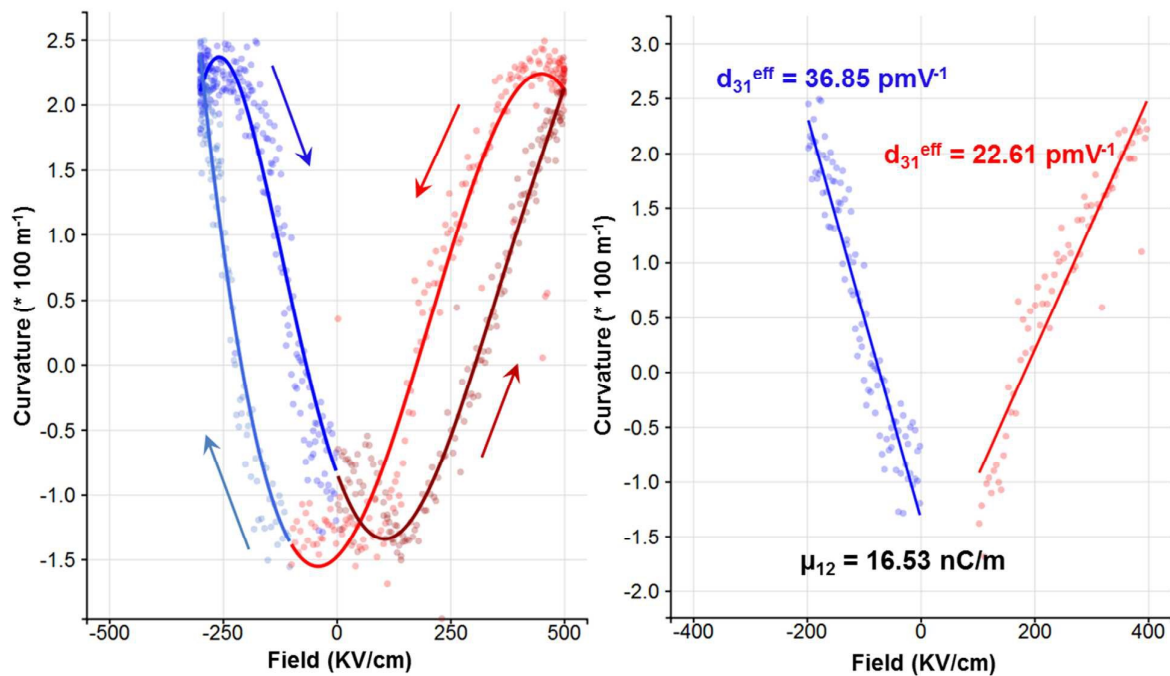
Figure 5 (a) Butterfly hysteresis loops of curvature as a function electric field for the 100 nm thick and PZT bimorph. In this case, a thick top electrode of SRO is used to partially compensate the non-centrosymmetric induced by the YSZ layer. The resulting structure results in larger asymmetry between piezoelectric coefficients. (b) Data from reverse sweeps (i.e., poled state) of curvature k as a function of the applied field.